

Sox2-Deficient Müller Glia Disrupt the Structural and Functional Maturation of the Mammalian Retina

Amelia R. Bachleda,^{*,1,2} Larysa H. Pevny,^{†,1,3} and Ellen R. Weiss^{1,4,5}

¹Neuroscience Center, University of North Carolina-Chapel Hill, Chapel Hill, North Carolina, United States

²Curriculum in Neurobiology, University of North Carolina-Chapel Hill, Chapel Hill, North Carolina, United States

³Department of Genetics, University of North Carolina-Chapel Hill, Chapel Hill, North Carolina, United States

⁴Department of Cell Biology and Physiology, University of North Carolina-Chapel Hill, Chapel Hill, North Carolina, United States

⁵Lineberger Comprehensive Cancer Center, University of North Carolina-Chapel Hill, Chapel Hill, North Carolina, United States

Correspondence: Ellen R. Weiss, Department of Cell Biology and Physiology, The University of North Carolina at Chapel Hill, Chapel Hill, NC 27599, USA; erweiss@med.unc.edu.

†Deceased September 30, 2012

Current Affiliation: *Institute for Learning & Brain Sciences, University of Washington, Seattle, Washington, United States

Submitted: August 19, 2015

Accepted: February 13, 2016

Citation: Bachleda AR, Pevny LH, Weiss ER. Sox2-deficient Müller glia disrupt the structural and functional maturation of the mammalian retina. *Invest Ophthalmol Vis Sci.* 2016;57:1488-1499. DOI:10.1167/iovs.15-17994

PURPOSE. Müller glia (MG), the principal glial cells of the vertebrate retina, display quiescent progenitor cell characteristics. They express key progenitor markers, including the high mobility group box transcription factor SOX2 and maintain a progenitor-like morphology. In the embryonic and mature central nervous system, SOX2 maintains neural stem cell identity. However, its function in committed Müller glia has yet to be determined.

METHODS. We use inducible, MG-specific genetic ablation of *Sox2* in vivo at the peak of MG genesis to analyze its function in the maturation of murine MG and effects on other cells in the retina. Histologic and functional analysis of the *Sox2*-deficient retinas is conducted at key points in postnatal development.

RESULTS. Ablation of *Sox2* in the postnatal retina results in disorganization of MG processes in the inner plexiform layer and mislocalized cell bodies in the nuclear layers. This disorganization is concurrent with a thinning of the neural retina and disruption of neuronal processes in the inner and outer plexiform layers. Functional analysis by electroretinography reveals a decrease in the b-wave amplitude. Disruption of MG maturation due to *Sox2* ablation therefore negatively affected the function of the retina.

CONCLUSIONS. These results demonstrate a novel role for SOX2 in glial process outgrowth and adhesion, and provide new insights into the essential role Müller glia play in the development of retinal cytoarchitecture. Prior to this work, SOX2 was known to have a primary role in determining cell fate. Our experiments bypass cell fate conversion to establish a new role for SOX2 in a committed cell lineage.

Keywords: vision, synapse formation

Müller glia (MG), the principal macroglia of the vertebrate retina, retain many stem cell characteristics. They are the last cell type to develop from multipotent retinal progenitor cells (RPCs). Retinal progenitor cells give rise to all six types of retinal neurons in a distinct spatio-temporal order spanning embryonic day (E)12 to postnatal day (P)10 in the murine retina.^{1,2} Born from P0 to P10, MG preserve RPC radial morphology spanning the apical/basal axis of the retina.³⁻⁵ Müller glia also retain an RPC-like gene expression profile, including the expression of SOX2, a high mobility group box transcription factor that maintains stem cell pluripotency in the embryonic nervous system and in populations of adult neural stem cells.⁶⁻¹⁰ While numerous studies have examined aspects of MG's neurogenic potential after injury,¹¹⁻¹⁴ a role for SOX2 in committed MG has not been defined.

We previously demonstrated that SOX2 is required for the maintenance of neurogenic potential in RPCs, as well as for maintaining early postnatal RPC/MG quiescence.^{15,16} Ubiquitous *Sox2* ablation in vitro in P0 RPCs results in aberrant MG cell cycle entrance at P5. This reentrance of nascent MG into the cell cycle results in their eventual depletion and the structural collapse of the retina by P10.¹⁶ These studies reinforce the well-established role *Sox2* plays in determining

cell fate. However, the functions of SOX2 in cell populations with determined cell fates like MG, which express SOX2 constitutively, remain largely unexplored. Over the first postnatal month, MG processes develop an intricate network that provides architectural support and enables MG to maintain retinal homeostasis.^{17,18} However, little is known about postnatal maturation of MG and the elaboration of their processes.¹⁹⁻²¹ Once this network is established, MG facilitate neuronal transmission by supporting glucose metabolism, ion and water homeostasis, recycling neurotransmitters, channeling light to the photoreceptors, and even retinal regeneration.^{4,22-26}

In this study, we address the role of SOX2 in MG function by characterizing the maturation of *Sox2*-deficient MG. We find that expression of SOX2 is essential for proper elaboration of the extensive side branches that MG develop during the first 2 postnatal months. Disruption in these processes results in loss of neuronal function as well as disruption of amacrine and horizontal cell neurites in the inner nuclear and outer plexiform layers (INL and OPL), respectively. These data indicate a new role for SOX2 in the maturation of MG, and provide insights into the role of these cells in the maintenance of retinal cytoarchitecture and function.

MATERIALS AND METHODS

Mouse Lines

All animal work was carried out in accordance with the University of North Carolina Institutional Animal Care and Use Committee and the ARVO Statement for the Use of Animals in Ophthalmic and Vision Research. Generation of the Sox2^{COND} mouse line was previously described²⁷; GLASTCreER mice were a gift from Jeremy Nathans, PhD.²⁸⁻³⁰ The Rosa26-Reporter strain³¹ (R26R) was obtained from Jackson Laboratories. All mouse lines in this study were maintained on a mixed CD1;C57BL6/J background. Genotyping primers and protocols were described previously.¹⁶

Sox2 Ablation

The line Sox2^{COND} was crossed to the glial specific, tamoxifen (TAM)-inducible GLASTCreER line, and to the R26R reporter line. Pregnant dams were monitored to determine pups' date of birth (P0). We gave P5 Sox2^{MUTANT} (Sox2^{COND/COND};GLAST-CreER;R26R) and Sox2^{CONTROL} (Sox2^{COND/+};GLASTCreER;R26R or Sox2^{+/+};GLASTCreER;R26R) pups a 60- μ L intragastric injection of 8 mg/mL tamoxifen (Sigma-Aldrich Corp., St. Louis, MO, USA) prepared in a 1:10 EtOH:corn oil solution.

Immunohistochemistry

Retinas were harvested at P15, P25, and P60. Eyes were removed from the animal immediately following cervical dislocation and fixed in 4% paraformaldehyde (PFA) in PBS for 20 minutes. Eyes were then removed from the PFA solution and placed in PBS for dissection. An incision was made in the cornea, through which the lens was gently removed. Eyecups were returned to 4% PFA in PBS overnight. Eyecups were sequentially immersed in 10%, 20%, and 30% sucrose in PBS, mounted in optical coherence tomography (OCT) medium (Tissue-Tek; Sakura Finetek, Torrance, CA, USA) and frozen at -80°C . Horizontal 14 to 16 μm cryostat sections were blocked in 10% goat serum in PBS, 1.0% Triton X-100 solution for at least 2 hours, and then incubated with primary antibodies in a solution containing 5% goat serum and 0.1% Triton X-100 in PBS overnight at 4°C . Following three 5-minute washes in PBS, tissue was incubated with secondary antibodies for 1 hour at room temperature.

The following antibodies and stains were used at the noted dilutions for this study: SOX2, rabbit polyclonal (1:2000; Merck Millipore, Billerica, MA, USA); SOX2 mouse monoclonal (1:100; R&D Systems, Minneapolis, MN, USA), cellular retinaldehyde-binding protein (CRALBP, 1:500; Abcam, Cambridge, UK); Glutamine Synthetase (GS, 1:1000; Merck Millipore); β -galactosidase (1:10,000; Molecular Probes, Eugene, OR, USA); SOX9 (1:1000; Merck Millipore); Calretinin (1:500; Merck Millipore); Neurofilament (1:5000; Hybridoma Bank, University of Iowa, Iowa City, IA, USA); glial fibrillary acidic protein (GFAP, 1:500; DAKO, Glostrup Municipality, Denmark); Cleaved Caspase 3 (1:250; Cell Signaling Technology, Inc., Danvers, MA, USA); goat anti-mouse IgG1 (AlexaFluor 488 conjugate, 1:2000), goat anti-rabbit IgG (AlexaFluor 488 conjugate, 1:2000), goat anti-mouse IgG2a (AlexaFluor 546 conjugate, 1:1000), goat anti-rabbit (AlexaFluor 546 conjugate, 1:1000), Hoechst 33258 (1:10000; Invitrogen, Carlsbad, CA, USA). Z-stack images were collected on a confocal scanning microscope (LSM 710; Carl Zeiss Microscopy, LLC, Thornwood, NY, USA), collapsed, and processed using graphic editing software (Adobe Photoshop; Adobe Systems, San Jose, CA, USA).

Electron Microscopy

Eyecups (P60) were prepared as described above and fixed for 1 week in a solution of 2% glutaraldehyde, 2% paraformaldehyde in 0.1% cacodylate buffer, pH 7.2. Semi-thin 0.5- μm sections through the central retina were stained with 1% methylene blue. Images were collected on an inverted microscope (Leica DMIRB; Leica Microsystems GmbH, Wetzlar, Germany) with a camera (Retiga SRV-1394; QImaging, Surrey, BC, Canada). Electron microscopy specimens were postfixed in a solution of 2% osmium tetroxide in 0.1% cacodylate buffer and embedded in Epon 812 resin. Sections were cut at 65-nm thickness using an electron microscope (CU7; Leica Microsystems GmbH) and contrast stained with a 2% uranyl acetate, 4% lead citrate solution. Ultrathin sections were visualized on a transmission electron microscope (JEM-1400; JEOL USA, Inc., Peabody, MA, USA) using a charge-coupled device camera (ORIOUS SC1000, 35-mm port; Gatan, Inc., Pleasanton, CA, USA).

Histologic Statistical Analysis

At least four retinas from independent litters were analyzed for each molecular marker unless otherwise noted. To determine Causes Recombination (CRE) efficiency, the number of SOX2-positive MG was counted in four nonconsecutive sections in the central retina of five Sox2^{MUTANT} and five Sox2^{CONTROL} retinas at P10. The average number of SOX2-positive MG in each of the five Sox2^{MUTANT} and five Sox2^{CONTROL} retinas was compared using a Student's *t*-test (2-tailed, heteroscedastic). The recombination percentage was calculated by dividing the average number of SOX2 positive MG cells in Sox2^{MUTANT} by the average number of SOX2-positive MG cells in Sox2^{CONTROL} retinas and subtracting that number from 1.

Retinal thickness was measured in three, nonconsecutive horizontal sections in five mutants and five controls. ImageJ (<http://imagej.nih.gov/ij/>; provided in the public domain by the National Institutes of Health, Bethesda, MD, USA) was used to determine the length of the retina from optic nerve head to the edge of the neural retina. The length of the retina was then trisected and the thickness of the retina was measured at inner (nearest to optic nerve), central, and peripheral points. Inner, central, and peripheral measurements for each of the three sections per retina were averaged and the values from the five Sox2^{CONTROL} and Sox2^{MUTANT} retinas were compared using an unpaired Student's *t*-test (2-tailed, homoscedastic).

Discontinuity in MG endfeet at the inner limiting membrane (ILM) was measured in three, nonconsecutive horizontal sections in five mutants and five controls. For each section, the number of gaps in glutamine synthetase (GS) staining at the ILM was measured. The number of gaps in GS staining for each of the three sections per retina was averaged and the values from the five Sox2^{CONTROL} and Sox2^{MUTANT} retinas were compared using an unpaired Student's *t*-test (2-tailed, heteroscedastic).

Pixel density in the inner plexiform layer (IPL) was measured in five 100 \times 100 pixel regions from six mutant and six litter-matched control retinas stained with GS at P25. Each pair of mutant and control images was taken with the same imaging parameters and stained in the same group. Using photo editing software (Adobe Photoshop; Adobe Systems), a square grid was applied to each image. Pixel density was measured in five 100 \times 100 pixel regions in the IPL for each image. The grid was used to determine which 100 \times 100 region to analyze. The first 100 \times 100 region measured for each region was aligned with the left side of the image in the *x*, or horizontal, axis. Vertically the 100 \times 100 region was in positioned as close to the ILM as possible without including

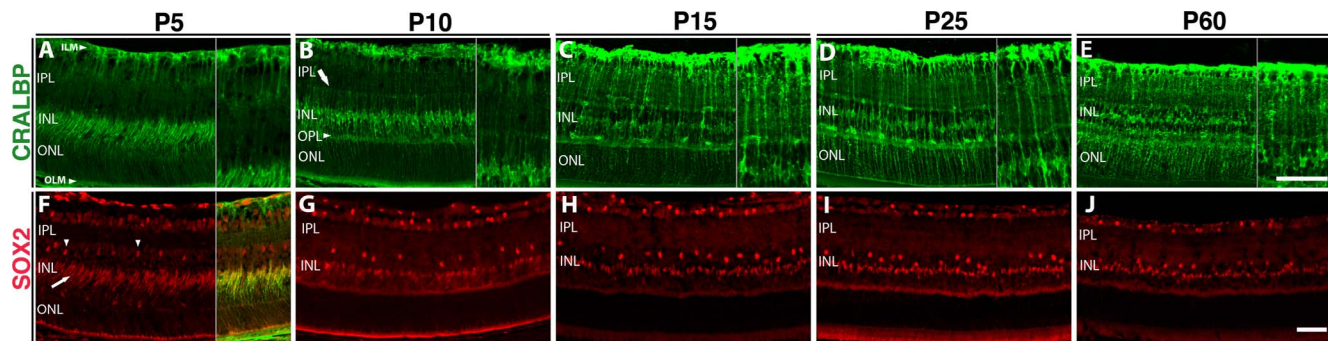


FIGURE 1. Müller glia mature slowly over the first postnatal month. (A–E) The Müller-specific marker CRALBP highlights morphologic maturation. (A) At P5, MG apicobasal processes are established at the inner and OLMs; *insets* show detail of the IPL, extending from the ILM to the INL. (B) At P10, MG extend side processes into the OPL (*arrowhead*) and define the boundary of the IPL (*arrow*). (C) At P15, MG display a marked increase in the density of processes: bands of MG fibers ensheathing neuronal processes in the IPL form, lamellar processes enveloping photoreceptor cell bodies are visible in the ONL. (D) At P25, Müller glial process in the IPL and ONL are well defined. (E) At P60, concomitant with slight decrease in retinal thickness, MG processes in IPL and ONL increase in density. (F–J) SOX2 stains MG and a subset of amacrine cells in the mature retina. (F) At P5, SOX2 is specifically expressed in the immature and elongated MG cell bodies in the INL (*arrow*) and a subpopulation of amacrine cells (*arrowheads*) in the INL. At P5, SOX2 expression is specifically colocalized with CRALBP expression (*inset*). (G) At P10, MG cell body morphology is mature and SOX2 staining is well defined. (G–J) SOX2 localization and expression in the INL remains static from P10 to P60. *Scale bar*: 50 μm .

dense staining from MG endfeet. Then moving from horizontally from left to right, a region of 100 pixels in length was skipped. The next 100×100 region was then measured. The left side of the bounding box placed at a distance of 200 pixels from the left side of the image. The top side of the bounding box was again aligned along vertical axis, positioned just below MG endfeet. This pattern was repeated until five regions for each image were measured. Median pixel density was measured using the histogram tool of the photo editing software (Adobe Systems). Median pixel intensities for each section were averaged. Pixel density values from the six Sox2^{CONTROL} and six Sox2^{MUTANT} retinas were compared. The hypothesis that the average pixel density values were higher in the IPL of Sox2^{CONTROL} retinas compared with Sox2^{MUTANT} retinas was tested using a paired Student's *t*-test (1-tailed, homoscedastic).

For the MG cell body analysis, *x*- and *y*-coordinates of SOX9-positive cells were obtained from six nonconsecutive sections in the central retina of five Sox2^{MUTANT} and five Sox2^{CONTROL} retinas at P25. We measured disorganization in the retina using a modified least squares analysis in which we measured the distance of each SOX9-positive MG cell body from a band representing a theoretical organized retina. The “organizational band” was defined as the region 19.5 μm (approximately the width of four MG cell bodies) above and below the quadratic least squares fit to the measured *x*- and *y*-coordinates of the MG cell bodies in each section of each retina. Mean squared distance from the edge of the organizational band was computed for each section and pooled to create a disorganization metric for each retina. Disorganization of control and mutant retinas was compared using a Student's *t*-test (2-tailed, heteroscedastic).

Electroretinography

Electroretinogram responses to light were recorded using an electroretinography system (Espion E² with ColorDome Ganzfeld Stimulator; Diagnosys LLC, Lowell, MA, USA). We dark-adapted P25 and P60 Sox2^{MUTANT} and Sox2^{CONTROL} animals overnight, then anesthetized them via intraperitoneal injection with 2.5% tribromoethanol (Avertin; Winthrop Laboratories, New York, NY, USA) at 0.018 mL/g and maintained at 37°C on a heated platform. Pupils were dilated with 2.5% phenylephrine hydrochloride and 1% tropicamide.

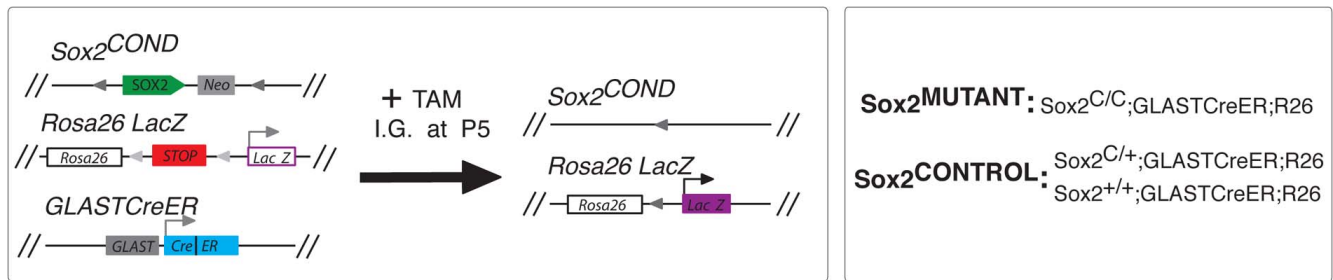
Hydroxypropyl methylcellulose was applied to the eyes to prevent dehydration. Electroretinograms were recorded under scotopic (dark-adapted) conditions in response to 12 flashes (4 ms in duration) of light intensities ranging from 0.001 to 100 scot cd/m². Traces from each eye were averaged across four flashes per intensity. The negative a-wave that arises from the photoreceptor response was calculated as the amplitude of the negative peak following the flash. The positive b-wave generated in the inner retina was calculated as the amplitude of the positive peak from the negative trough of the a-wave. The data were graphed using graphing and statistics software (Graphpad Prism; GraphPad Software, Inc., La Jolla, CA, USA). Amplitudes of P25 a- and b-wave from 14 Sox2^{MUTANT} and 12 Sox2^{CONTROL} eyes were compared using a Student's *t*-test at each step; statistical significance was determined using the Holm-Sidak method, with alpha = 5.000%.

RESULTS

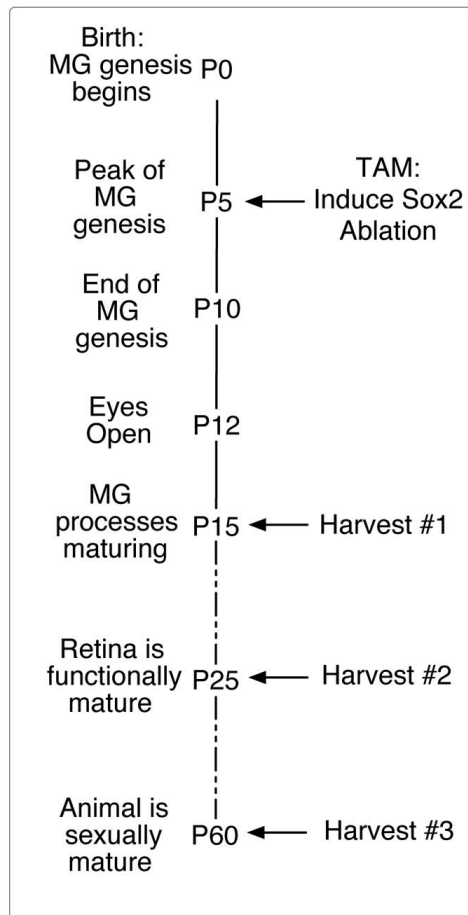
Müller Glia Mature Throughout the First Postnatal Month

We analyzed the maturation process of Müller glia in wild-type mice over the first 2 postnatal months using the Müller glial marker, CRALBP, a protein involved in chromophore transport³² (Fig. 1A). At P5, the main apicobasal processes are well established and MG endfeet at the inner and outer limiting membranes (OLMs) have been formed. Müller glia have not yet extended processes into the synaptic and neuronal layers. This is especially striking in the IPL (Fig. 1A, inset) and the outer nuclear layer (ONL). At this developmental stage, SOX2 is specifically expressed in MG cell bodies in the inner nuclear layer (INL) (Fig. 1F, arrow), where it colocalizes with CRALBP (Fig. 1E, inset), and cholinergic amacrine cells³³ (arrowheads) in the INL (Fig. 1F). At P10, just prior to eye opening, retinal synapses are forming.³⁴ At this stage, Müller glia have begun to extend side processes into the outer plexiform layer (OPL, arrowhead) and to define the outer boundary of the inner plexiform layer (IPL; Fig. 1B, arrow). The SOX2 staining in the elongated Müller cell bodies is well defined (Fig. 1G). By P15, there is a considerable increase the density of processes (Fig. 1C) and the bands of MG fibers that ensheath neuronal processes in the IPL are beginning to form. In the ONL, definition in the lamellar processes that envelope the

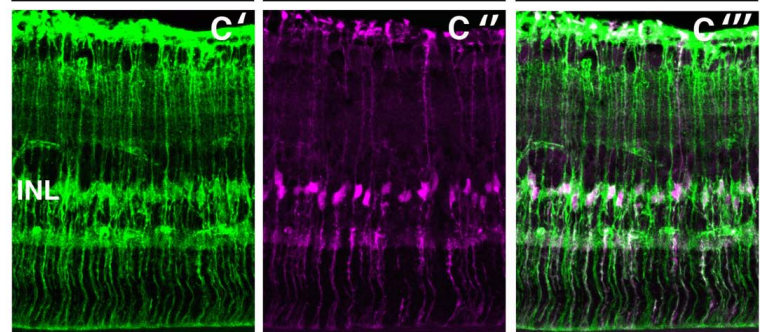
A Alleles



B MG Maturation



C Glutamine Synthetase β-galactosidase GS β-gal



D SOX2 β-galactosidase SOX2 β-gal

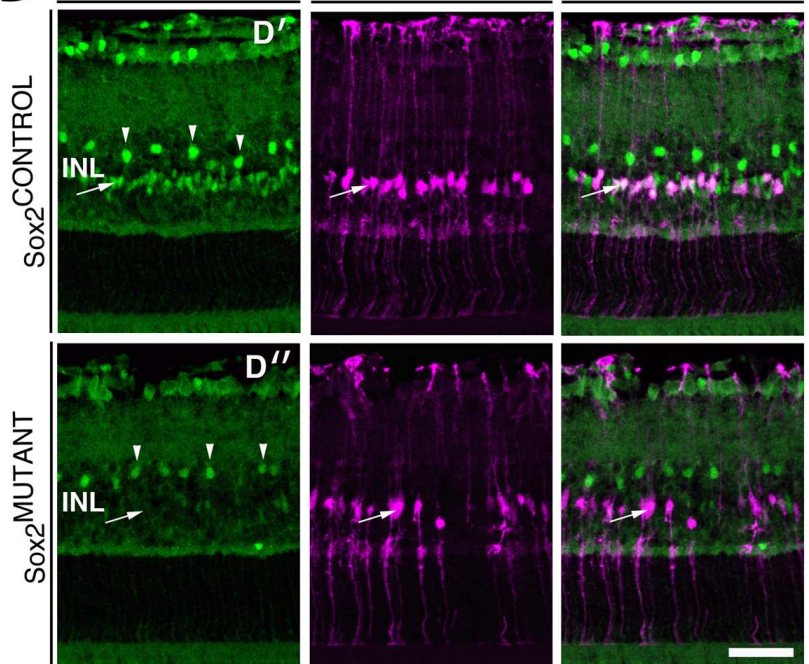


FIGURE 2. Robust MG-specific *Sox2* ablation. **(A)** Genetic ablation of *Sox2* in postnatal MG using the *Sox2* conditional mouse. The *Sox2*^{COND} allele contains the *Sox2* open reading frame flanked by loxP sites. The *Sox2*^{COND} line was crossed to a glial specific, TAM-inducible Cre line, GLASTCreER, and to the Rosa26LacZ reporter line. Tamoxifen was administered via intragastric injection at P5, resulting in deletion of the *Sox2* coding sequence and expression of β-galactosidase in *Sox2*^{MUTANT} populations. **(B)** Experimental timeline; *Sox2* ablation was induced at P5; retinas were harvested at P15, P25, and P60. **(C)** Expression of GLASTCRE is MG specific; the MG marker glutamine synthetase (C') and Cre induced β-galactosidase staining (C'') are coexpressed in P15 MG (C'''). **(D)** Following TAM administration, SOX2 staining is absent from *Sox2*^{MUTANT}-MG cell bodies in the INL (D'', arrow), but maintained the population of SOX2-positive amacrine cells (typified by cells at arrowheads) in both *Sox2*^{MUTANT} (D'') and *Sox2*^{CONTROL} (D') retinas at P15. At P10, the efficiency of CRE recombination in *Sox2*^{MUTANT} MG is 83% ($P < 0.0001$, $n = 5$). Scale bar: 50 μm.

photoreceptor cell bodies is now evident. At P25, synaptogenesis is complete and Müller glial processes in the IPL and ONL are well defined (Fig. 1D).^{4,34} However, further maturation of MG processes is observed from P25 to P60. Concomitant with

a slight decrease in the thickness of the retina is an increase in density of the MG processes in both the IPL and ONL (Fig. 1E). Expression of SOX2 in the INL reveals that the morphology and localization of MG cell bodies remains relatively stationary

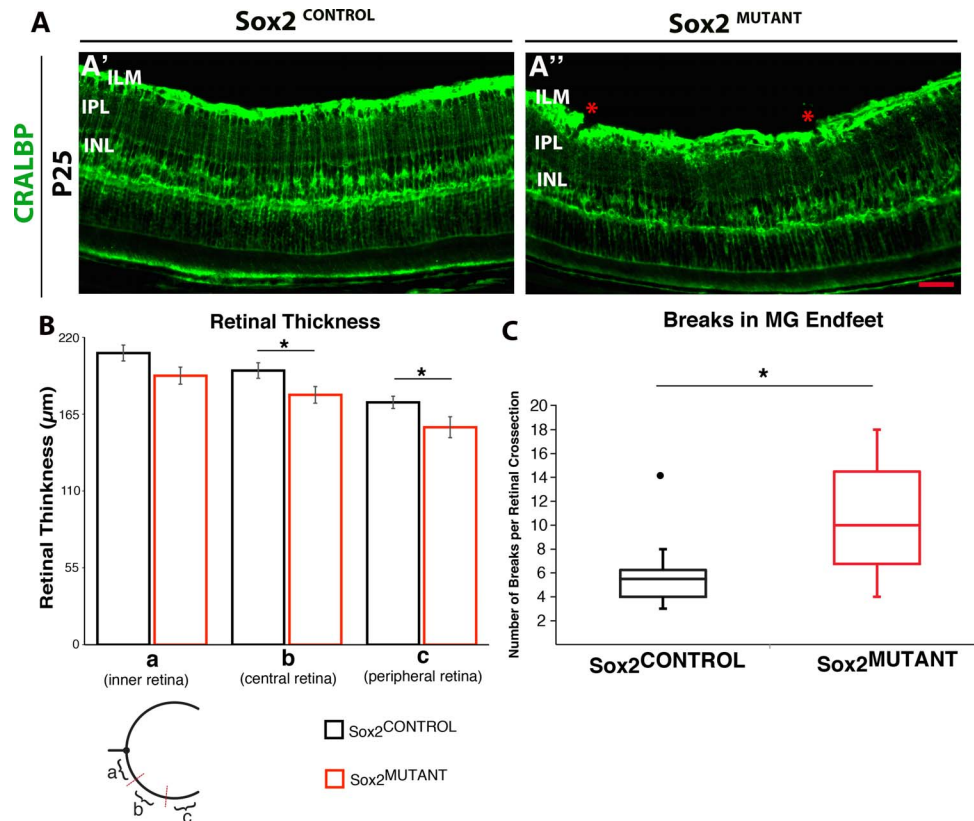


FIGURE 3. *Sox2* ablation reduces retinal thickness and results in disruption of the MG endfeet at the ILM at P25. (A) Staining of CRALBP demonstrates MG processes in the IPL are disorganized and their endfeet at the ILM are disrupted in *Sox2*^{MUTANT} compared with *Sox2*^{CONTROL} retinas. This phenotype was quantified in retinas stained with MG-specific GS. (B) The central and peripheral retina is significantly reduced in thickness in the *Sox2*^{MUTANT} compared to *Sox2*^{CONTROL} (average retinal thicknesses of the central retina 179 µm [SD ± 12] and 196 µm [SD ± 11], respectively, and the average retinal thicknesses of the peripheral retina is 156 µm [SD ± 15] and 173 µm [SD ± 9], respectively $n = 5$). **P* values are: inner, 0.06; central, 0.04; peripheral, 0.05. (C) *Sox2*^{CONTROL} retinas had significantly fewer disruptions of the MG endfeet compared to *Sox2*^{MUTANT} retinas stained with GS (Average number of disruptions is 6 [SD ± 1.5] and 11 [SD ± 10.8], respectively $n = 5$). **P* = 0.05. The • symbol in *Sox2*^{CONTROL} represents a single outlying value not included in the statistical comparison. If the outlier is included, *P* = 0.07.

from P10 to P60 (Figs. 1G–J). These data point to an active and extensive period of postnatal MG maturation in the murine retina.

Müller Glia-Specific *Sox2* Ablation

To determine the function of SOX2 in the maturation of MG *in vivo*, we genetically ablated *Sox2* in postnatal MG using a *Sox2* conditional mouse line previously generated by our laboratory²⁷ (Fig. 2A). The *Sox2*^{COND} line was crossed to a glial specific, TAM-inducible Cre line, GLASTCreER²⁹ and to the Rosa26LacZ reporter line.³¹ Administration of a systemic dose of TAM to the *Sox2*^{COND/COND};GLASTCreER;R26R pups (“*Sox2*^{MUTANT}”; Fig. 2A) results in efficient, MG-specific, *Sox2* ablation in the postnatal retina (Fig. 2D’ compared with Fig. 2D”) at P15). Figure 2B outlines the protocol used to assess the role of SOX2 in the maturation of Müller glia. Ablation of *Sox2* was induced at P5, which is the height of Müller glia genesis in the murine retina.⁵ Retinas were harvested at P15 during the maturation of Müller glial processes, at P25 when the retina is functionally mature and synaptogenesis is complete,^{4,34} and at P60, when MG maturation appears to be complete in wild-type animals (Fig. 1E). Induction of CRE expression by tamoxifen administration at P5 results in robust, MG-specific CRE expression at P15, as shown by colocalization of β-galactosidase (β-gal) and the MG marker glutamine synthetase (Fig. 2C). *Sox2* is specifically ablated in

Sox2^{MUTANT}-MG cell bodies located in the INL (arrow) (Fig. 2D”). The efficiency of CRE recombination at P10 in *Sox2*^{MUTANT} MG is 83%, based on a comparison of the number of SOX2-positive cells in *Sox2*^{MUTANT} retinas with SOX2-positive cells in the *Sox2*^{CONTROL} retinas (Fig. 2D’). A population of SOX2-positive amacrine cells in the INL border maintains SOX2 expression in both *Sox2*^{CONTROL} and *Sox2*^{MUTANT} retinas (arrowheads; Fig. 2D’, 2D”). The establishment of this line allows for the genetic dissection of SOX2’s role in postnatal Müller glial maturation.

Loss of SOX2 Disrupts the Typical Maturation of MG Processes

Retinas from P25 *Sox2*^{MUTANT} and *Sox2*^{CONTROL} mice were stained with CRALBP and compared for changes in MG morphology (Fig. 3). The images in Figure 3A demonstrate that the MG processes in the *Sox2*^{MUTANT} IPL are less organized with respect to the density of processes compared with control (Figs. 3A’, A”). Retinal thickness was quantified in retinas stained with MG-specific glutamine synthetase (GS) at P25 and results indicate that the mutant retinas are consistently thinner (Fig. 3B). While significant in the central and peripheral retina, the effect was modest. The integrity of the MG endfeet at the ILM is also disrupted (see asterisks in Fig. 3A”). The disruption of the MG endfeet was severe, resulting in a significant level of discontinuity MG endfeet in sections

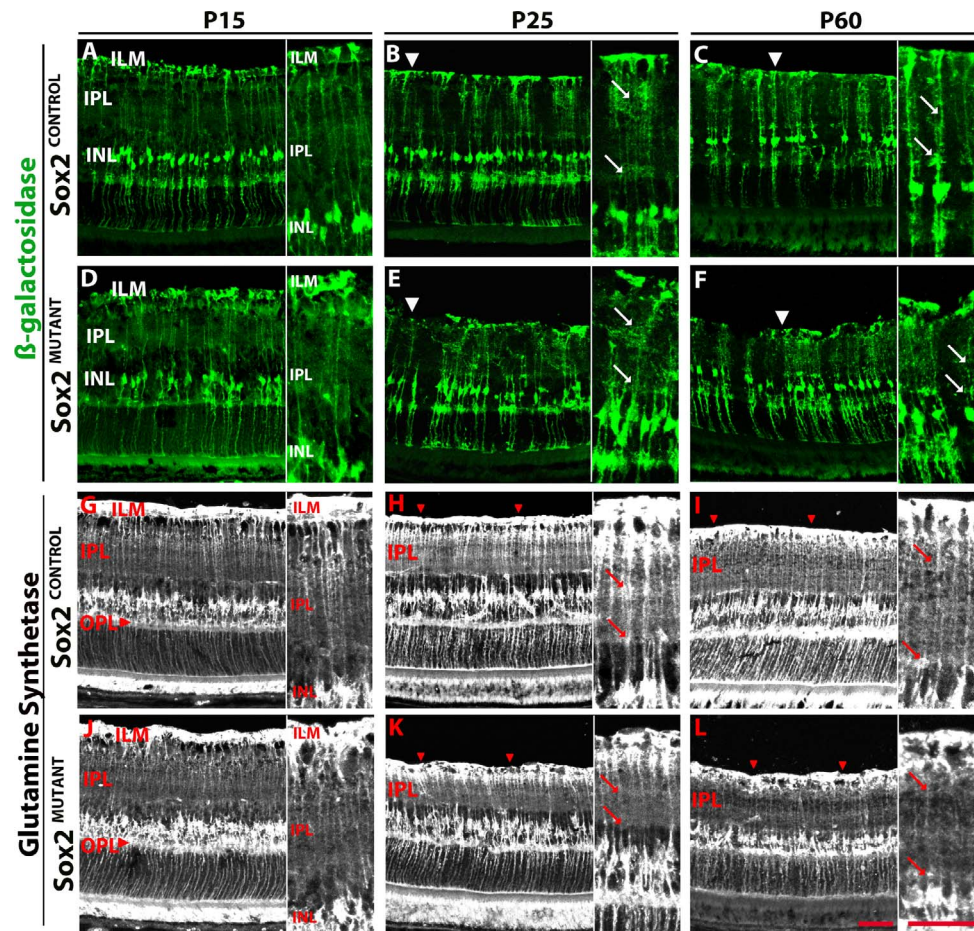


FIGURE 4. Disorganization of Sox2^{MUTANT} Müller glia processes progresses developmentally. (A–F) Müller glia that are CRE positive express β -galactosidase. (A, D) At P15, Sox2^{MUTANT} (D, inset) and Sox2^{CONTROL} (A, inset) MG processes in the IPL display similar morphologies. (B, E) At P25, Sox2^{MUTANT} (E, inset, arrows) MG side processes are disorganized in the IPL compared with Sox2^{CONTROL} (B, inset, arrows). Müller endfeet at the ILM are disrupted in the Sox2^{MUTANT} (E, arrowhead). (C, F) At P60, MG processes in the IPL and ILM remain diffuse and disorganized in the Sox2^{MUTANT} (F, inset) compared with Sox2^{CONTROL} (C, insets). (G–L) Glutamine synthetase labeling of the entire MG population. (G, J) At P15, the Sox2^{MUTANT} (J, inset) and Sox2^{CONTROL} (G, inset) processes in the IPL have a similar morphology. Sox2^{MUTANT} processes in the OPL expand into a greater area compared with control (G, J, arrowheads). (H, K) At P25, Sox2^{MUTANT} MG processes in IPL (K, inset) are significantly decreased in density compared to control (H, inset); arrows denote a decreased density of processes that define the INL border and the synaptic bands in the IPL. Randomized quantification of the pixel density of the IPL demonstrates that the density of processes in the IPL is 1.3-fold higher in the control compared with the mutant retinas ($P=0.03$). Disruptions in the MG endfeet are present in the Sox2^{MUTANT} (arrowheads). At P60, disruptions in the Sox2^{MUTANT} (L, inset) IPL, OPL, and MG endfeet compared with Sox2^{CONTROL} (I, inset) are maintained. Scale bar: 50 μ m.

stained with GS (Fig. 3C). This quantification of the disruptions mirrors the disruptions visualized at the ILM in the mutant stained with CRALBP in Figure 3A.

To examine the SOX2-negative MG population over the course of their postnatal maturation, the CRE-positive MG population was identified via β -galactosidase staining at P15, P25, and P60 (Fig. 4). At P15, Sox2^{MUTANT} and Sox2^{CONTROL} Müller glia processes in the IPL display similar morphologies (Figs. 4A, 4D; insets). However, by P25, a visible disorganization of MG side processes in the Sox2^{MUTANT} IPL is evident (Figs. 4B, 4E; insets, arrows). As described in Figure 3, the Müller glial endfeet at the ILM also appear disrupted in the mutant (Figs. 4B, 4E; arrowheads refer to MG endfeet at the ILM). At P60 Müller glial processes in the IPL and ILM remain disorganized compared with processes in Sox2^{CONTROL} retinas (Figs. 4C, 4F; arrows in insets at ILM). These data indicate that ablation of SOX2 in Müller glia at P5 results in aberrant maturation and development of processes by P25.

We also examined the entire population of Müller glia at P15, P25, and P60 (Figs. 4G–L) by looking at the expression

pattern of GS to visualize the density of processes in the synaptic layers and the integrity of the MG endfeet at the inner and outer limiting membranes over the course of MG maturation. As shown in Figure 1, MG processes in the IPL undergo significant maturation during the first 2 postnatal months. At P15, Müller glial apicobasal processes in the IPL of the Sox2^{MUTANT} retinas are similar in morphology to the control (compare the insets in Figs. 4G, 4J). However, Sox2^{MUTANT} processes that extend into the outer plexiform layer (OPL) are not as organized at the OPL/ONL border compared with control retinas (Figs. 4G, 4J; arrowheads). By P25, there is a marked and significant decrease in density and complexity of MG processes in IPL of the Sox2^{MUTANT} (Fig. 4K) compared with control retinas (Fig. 4H) as described in Figure 3B. Particularly evident in the insets is the decreased density of processes that define the INL border and synaptic bands in the IPL (arrows indicate regions of decreased density; insets for Figs. 4H, 4K). Quantification of this phenotype was conducted in P25 retinas stained with GS. Randomized quantification of the pixel density of the IPL demonstrates that the density of

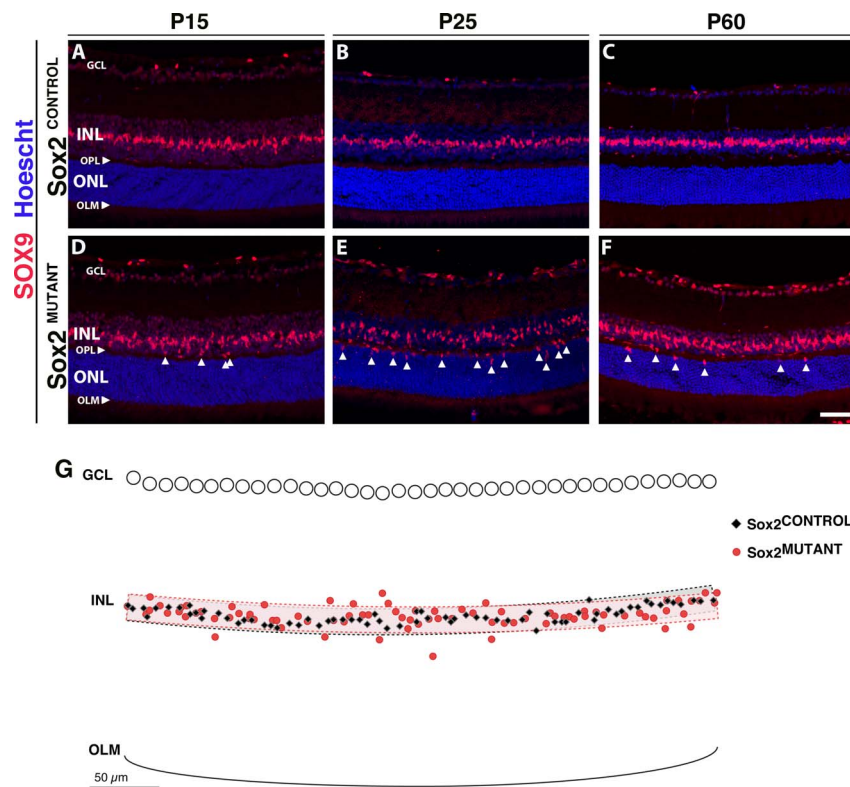


FIGURE 5. Sox2^{MUTANT}-Müller glial cell bodies are disorganized. (A–F) Müller glial cell bodies in the INL are specifically labeled with SOX9. (A, D) At P15, Sox2^{MUTANT} MG (D) have mislocalized cell bodies compared with Sox2^{CONTROL} (A), with some nuclei located ectopically in the OPL and the ONL (D, arrows). (B, E) At P25, Sox2^{MUTANT}-MG cell bodies (E, arrows) display increased disorganization compared with Sox2^{CONTROL} (B). Significant INL disorganization of Sox2^{MUTANT}-MG cell bodies was identified by a least squares regression analysis ($P = 0.042$, $n = 5$ eyes). (G) Exported and overlaid (x , y) coordinates of a representative P25 Sox2^{MUTANT} and Sox2^{CONTROL} pair with graphical representation of the organizational bands used in the analysis. (C, F) At P60, Sox2^{MUTANT} SOX9-positive MG remain disorganized (F, arrows) compared with Sox2^{CONTROL} (C), and are decreased in number compared to the P25 Sox2^{MUTANT} (E). Scale bar: 50 μm . Hoescht dye was used to stain the nuclei (blue).

processes in the IPL is 1.3-fold higher in the control compared with the mutant retinas ($P = 0.03$). Disruptions in the MG endfeet at the ILM (also seen in the β -galactosidase staining in Figs. 4D, 4E, and CRALBP staining in Fig. 3), are clearly present in the Sox2^{MUTANT} (the ILM is marked by arrowheads; Figs. 4H, 4K). The reduced density of processes in the Sox2^{MUTANT} IPL and disrupted OPL and ILM are even more apparent at P60 (Figs. 4I, 4L) suggesting that this phenotype progresses over the course of MG maturation and that once disrupted, Müller glial morphology does not return to normal.

Displacement of MG Cell Bodies Due to Sox2 Ablation

To define and quantify the disorganization of the MG in Sox2^{MUTANT} retinas, we examined SOX9 expression. In the INL, SOX9 specifically labels MG cell bodies. Compared with the control, the Sox2^{MUTANT} Müller glia have mislocalized cell bodies, with some nuclei located ectopically in the OPL and ONL, amid the photoreceptor cell bodies (Fig. 5). At P15, there is limited disorganization of Sox2^{MUTANT}-MG cell bodies (Figs. 5A, 5D; arrowheads indicate ectopic cell bodies). In contrast, at P25, there is a significant disorganization of Sox2^{MUTANT}-MG cell bodies ($P = 0.042$; Figs. 5B, 5E; arrowheads). The exported x - and y -coordinates of a representative P25 mutant and control pair are overlaid in Figure 5G along with graphical representations of a bands representing a theoretical organized retina as described in the Methods. At P60, SOX9-positive cells are still present in the ONL of the Sox2^{MUTANT} retina (Figs. 5C, 5F). The

mislocalization of Sox2^{MUTANT}-MG cell bodies shown in Figure 5 phenocopies MG disorganization that occurs during retinal degeneration.³⁵ However, cleaved caspase-3 and GFAP levels are not upregulated (data not shown). Therefore, these data provide evidence that the Sox2^{MUTANT} phenotype is a result of aberrant maturation rather than degeneration.

SOX9 also stained a population of cells, localized to the ganglion cell layer (GCL), which appeared to increase with age in the Sox2^{MUTANT} retinas. Previous work by others³⁶ suggests that these cells are astrocytes. The astrocytes participate in directing the ganglion cell axons toward the optic nerve. They also serve to ensheath the blood vessels and are thought to contribute to the blood/retina barrier in the inner retina.³⁷

Ablation of Sox2 in Müller Glia at P5 Disrupts Synaptic Layer Formation

Because the role of the MG is critical for support of the retinal neurons, the disorganization of MG processes in the IPL and OPL may lead to disruption of axons and dendrites in the plexiform layers. We therefore examined amacrine and ganglion cell neurites in the IPL and horizontal cell neurites in the OPL. A subset of amacrine cells, displaced amacrine cells, retinal ganglion cells, and three distinct bands of processes in the IPL are labeled with an antibody to the calcium binding protein, calretinin (Figs. 6A–F). The outer and inner bands of processes in the IPL are the cholinergic strata, while the middle band includes processes from nitric oxide synthase positive amacrine cells.³⁸ At P25, the Sox2^{MUTANT}

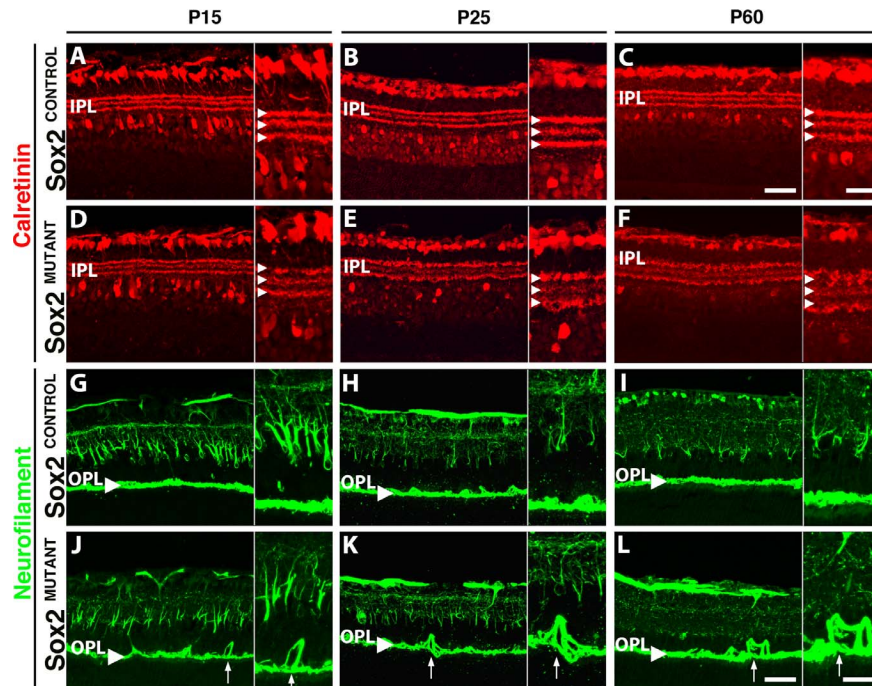


FIGURE 6. Sox2^{MUTANT} neuronal processes are disrupted. (A–F) The inner band of calretinin positive amacrine cell neurites is disrupted in the IPL of Sox2^{MUTANT} retinas (A–C) compared with Sox2^{CONTROL} retinas (D–F). At P25, Sox2^{MUTANT} ([E], *inset*) retinas display marked disorganization of amacrine neurites compared with Sox2^{CONTROL} ([B], *inset*) and compared with Sox2^{MUTANT} retinas at P15 (A, B). (C, F) At P60, the level of disruption of the IPL in Sox2^{MUTANT} compared with Sox2^{CONTROL} retinas is maintained. (G–L) Neurofilament-positive horizontal cell processes (G, *arrowhead*) are disrupted in the OPL of Sox2^{MUTANT}. (G, J) At P15, Sox2^{MUTANT} neurites (J, *inset*) are disorganized compared with Sox2^{CONTROL} (G), extending into the inner and ONLs (*arrow*). Disruption of the OPL is maintained in P25 and P60 Sox2^{MUTANT} (K, L; *arrows*) retinas compared with Sox2^{CONTROL} (H, I). *Scale bar*: main figures, 50 μ m; *insets*, 25 μ m.

retinas exhibit a disruption of the middle horizontal band of processes compared with the inner and outer bands. In contrast, all three bands in the control display similar organization (Figs. 6B, 6E; arrowheads in insets). The central band divides the IPL into the ON and OFF sublamina.³⁹ The disorganization of the amacrine cell processes is maintained at P60 (Figs. 6C, 6F), suggesting a stable phenotype from P25 onward. This phenotypic progression provides evidence that loss of SOX2 not only affects MG maturation, but also results in the abnormal development of neuronal processes and points to an extended period of neuronal maturation and plasticity in the postnatal retina.

Horizontal cells extend their processes into the OPL (Fig. 6G, arrowhead).⁴⁰ Neurofilament staining³⁸ reveals disruption of horizontal cell neurites, extending into the inner and outer nuclear layers in the Sox2^{MUTANT} at P15 (Fig. 6J, arrow). These disruptions are also observed at P25 (Figs. 6H, 6K, arrow at OPL) and P60 (Figs. 6I, 6L, arrow at OPL) in the Sox2^{MUTANT} retinas. The sprouting of horizontal cell processes has been observed previously in retinas that undergo remodeling or degeneration.^{41,42} Since, as noted above, no degeneration is observed in these mutant retinas, the disruption of amacrine and horizontal cell processes suggests impaired retinal maturation due to remodeling of the retina that occurs when MG are unable to stabilize these processes.

Disruptions in the outer retina were assessed using semi-thin section histology and electron microscopy. In the typical murine ONL, photoreceptor (PR) cell bodies form linear columns that are surrounded by MG lamellar processes (Fig. 7A, inset). However, in the Sox2^{MUTANT}, the columns of PR cell bodies are disorganized (Fig. 7B, inset). Furthermore, the OLM (arrows), formed by zonula adherens junctions between MG and photoreceptor cell bodies, is irregular in the

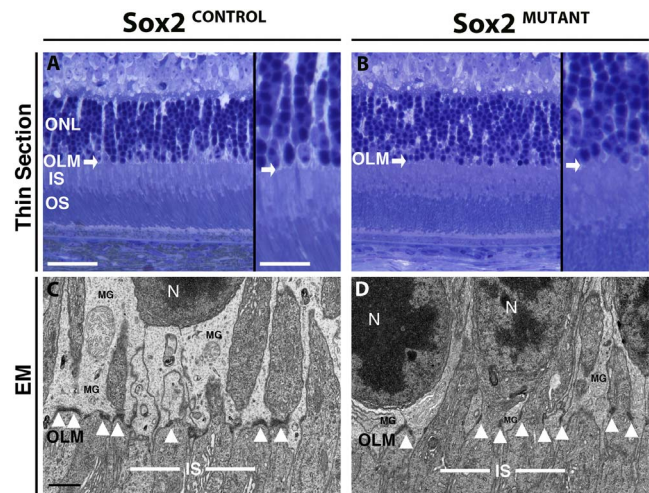


FIGURE 7. Sox2^{MUTANT} retinas display disruption of junctional complexes at the OLM. (A, B) Semi-thin sections through the outer retina highlight linear rows of PR nuclei in the ONL of the Sox2^{CONTROL} (*inset*). In the Sox2^{MUTANT} (*inset*) the rows of PR nuclei are formed irregularly. The outer limiting membrane (*white arrows*) formed between MG and photoreceptor outer segments is irregular in the Sox2^{MUTANT} compared with Sox2^{CONTROL}. (C, D) Electron micrographs show a reduced area of MG lamellar processes in Sox2^{MUTANT} (D) ONL, resulting in photoreceptor nuclei located approximately 2 μ m closer to the OLM compared with control (C). Zonula adherens junctions (*black arrowheads*) between MG and PR are irregularly formed in the Sox2^{MUTANT} (D) compared with Sox2^{CONTROL} (C). *Scale bars* (thin sections): main figures, 50 μ m; thin section insets, 25 μ m; *n* = 4 eyes for each condition. *Scale bar* (EM): 1.0 μ m, *n* = 3 Sox2^{MUTANT} eyes and *n* = 2 Sox2^{CONTROL} eyes.

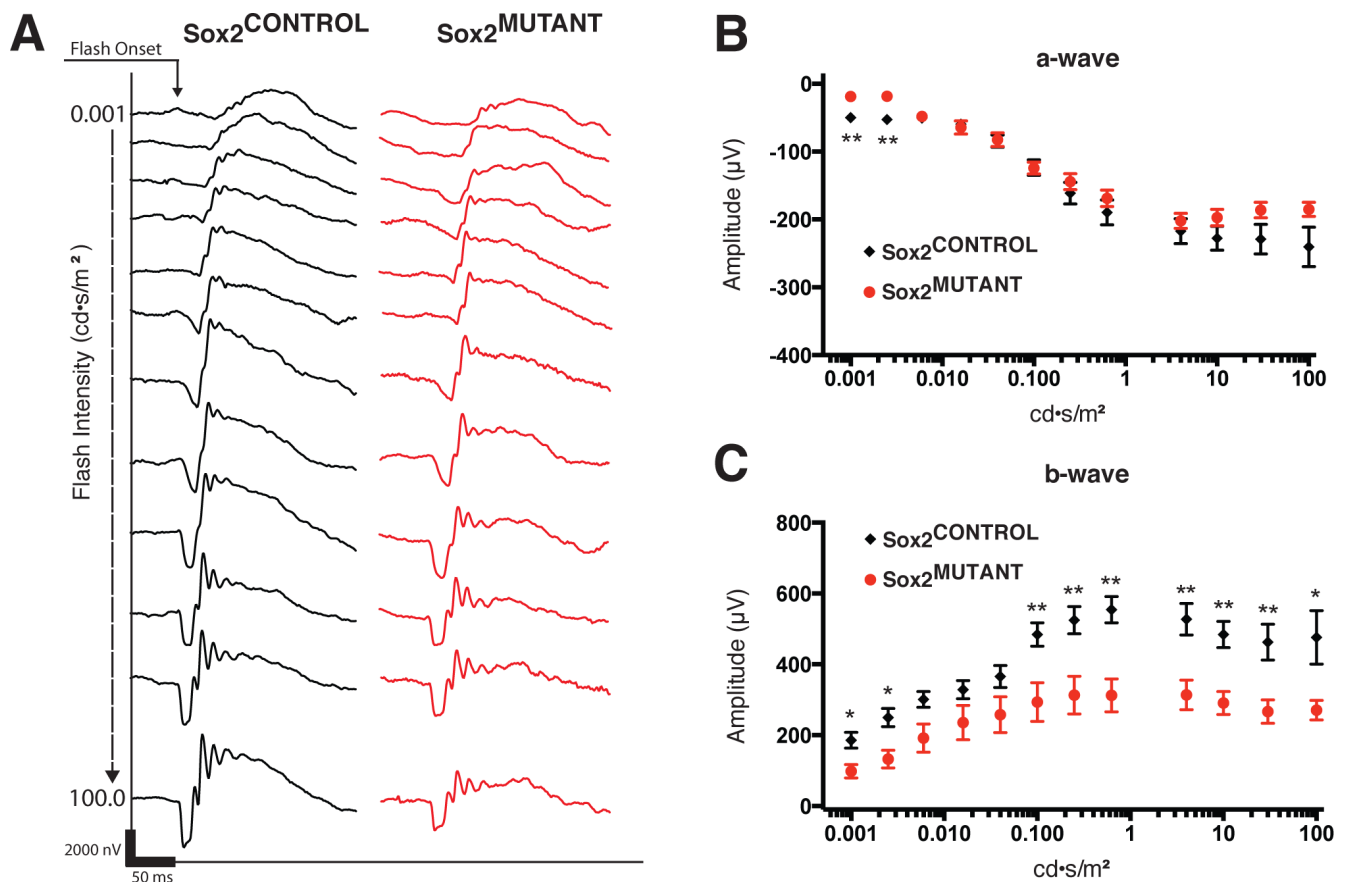


FIGURE 8. Loss of SOX2 in MG results in a deficit in retinal function. Electrophysiology at P25 demonstrates reduced function in Sox2^{MUTANT} retinas (A–C). (A) Representative traces from Sox2^{MUTANT} ($n = 14$) and Sox2^{CONTROL} ($n = 12$) eyes recorded under scotopic conditions in response to 12 flashes (4 ms in duration) of increasing light intensities ranging from 0.001 to 100 scot cd/m². (B) Sox2^{MUTANT} retinas show a significant decrease in a-wave amplitude at low light levels, indicating a decrease in rod function (step 1, $P = 0.0001$; step 2, $P = 0.0018$). Impaired cone function is suggested by a trend toward a decreased a-wave amplitude at the highest flash intensity ($P = 0.068$). (C) Sox2^{MUTANT} retinas display a highly significant reduction in b-wave amplitude over a range of low and high flash intensities, indicating functional disruption of the inner retina (step 1, $P = 0.0059$; step 2, $P = 0.0034$; step 3, $P = 0.0316$; step 4, $P = 0.1228$; step 5, $P = 0.0922$; step 6, $P = 0.0083$; step 7, $P = 0.0047$; step 8, $P = 0.0006$; step 9, $P = 0.0019$; step 10, $P = 0.0006$; step 11, $P = 0.0029$; step 12, $P = 0.0124$). * $P < 0.05$. ** $P < 0.01$.

Sox2^{MUTANT}, compared with the linearly formed OLM in the Sox2^{CONTROL}. At the ultrastructural level, the adherens junctions that form the OLM are identified as short (~0.3 μ m), dark densities between MG lamellar processes and photoreceptor cell bodies (arrowheads, Fig. 7C). In the Sox2^{MUTANT}, adherens junctions are visibly shorter and oriented parallel to the apical/basal axis of the retina as opposed to perpendicular in the Sox2^{CONTROL} (arrowheads, Fig. 7D). In the Sox2^{CONTROL}, MG processes maintain rod nuclei (RN) at a distance of approximately 3 μ m from the OLM. However, in the Sox2^{MUTANT}, these nuclei have collapsed basally to the edge of OLM similar to the observations in the thin sections (Fig. 7B). These observations provide evidence that the loss of SOX2 disrupts neuronal and glial processes throughout the entire width of the retina.

Loss of SOX2 in Müller Glia Results in Decreased Retinal Function

Electroretinograms were performed at P25 to assess retinal function in Sox2^{MUTANT} and Sox2^{CONTROL} retinas. Electroretinogram responses were recorded under scotopic (dark-adapted) conditions with a series of 12 light flashes (4 ms in duration) over a 10⁵-fold range of intensities. Representative traces from

Sox2^{CONTROL} and Sox2^{MUTANT} eyes are shown in black and red, respectively (Fig. 8A). At P25, ablation of Sox2 in Müller glia results in a significant decrease in a-wave amplitude at low light levels (Fig. 8B), indicating a minor decrease in rod function. Also notable is a decreasing trend in a-wave amplitude at the highest flash intensity, indicating a possible reduction in cone function. A highly significant reduction in b-wave amplitude was observed at low and high flash intensities (Fig. 8C). Postnatal day 60 retinas maintained a similar functional deficit as that observed at P25 (data not shown), consistent with histologic data. These data show that loss of SOX2 in MG disrupts not only the morphology of the neural retina and plexiform layers, but also results in a significant decrease in retinal function across a range of light intensities. Furthermore, these results demonstrate an essential function of MG to establish and stabilize the neuronal circuitry of the retina.

DISCUSSION

Loss of SOX2 in Müller Glia Disrupts Neuronal Structure and Function

Prior to our work, SOX2's essential role in the retina was known to be in specification of cell fate. By ablating Sox2 at P5,

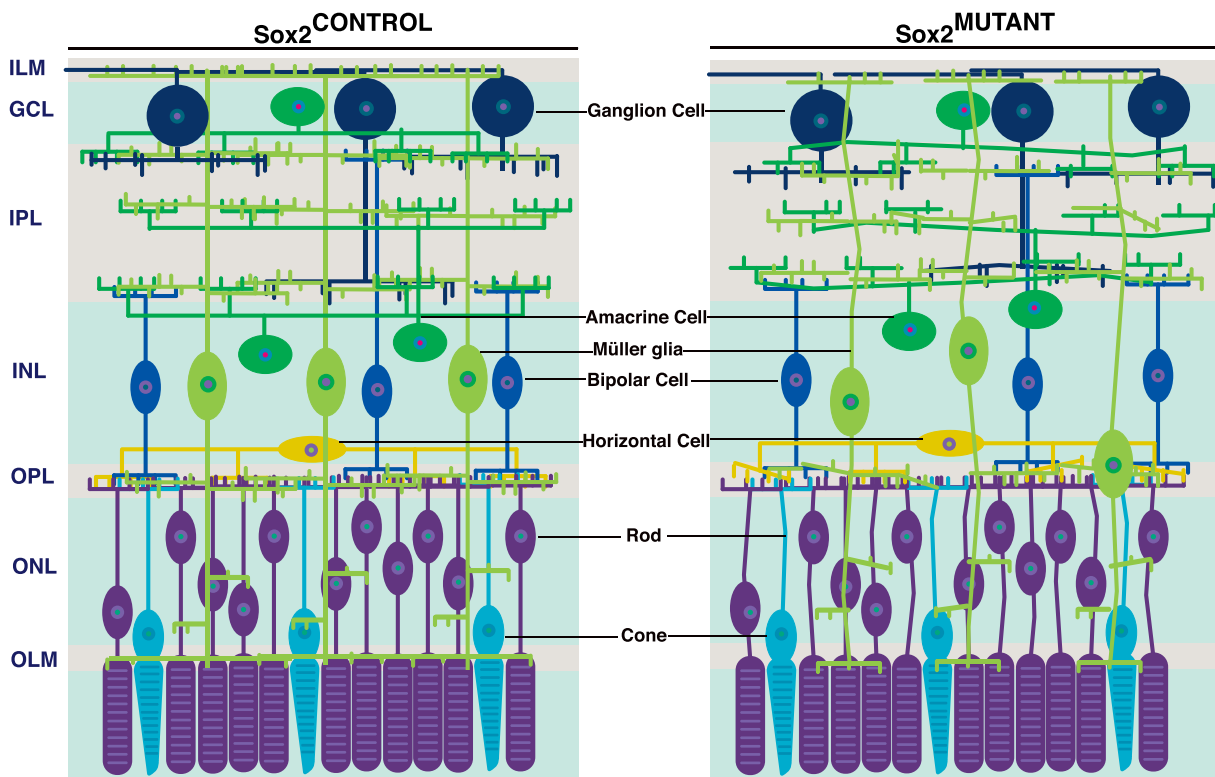


FIGURE 9. *Sox2* ablation in P5 MG results in their aberrant maturation. In the *Sox2*^{MUTANT} retina, disrupted Müller and neuronal processes are evident throughout the retina. The branching side processes of MG that extend into the inner and outer plexiform layers are disorganized and decreased in density. As maturation progresses, MG cell bodies in the *Sox2*^{MUTANT} retinas may be displaced from the inner nuclear layer when the appropriate architecture and density of lamellar processes fail to develop. Müller glial endfeet at the outer and inner limiting membranes are also disrupted and there is evidence of disrupted neural-glia adhesion. Neurites of amacrine cells in the inner plexiform and horizontal cells in the outer plexiform layer are disorganized. In the outer nuclear layer, photoreceptor cell bodies are also disorganized.

specifically in immature yet committed MG, therefore bypassing cell fate conversion, we have identified a novel role for this transcription factor in Müller glia process outgrowth, neuronal maturation and adhesion. Unlike *Sox2* ablation in RPCs, ablation in committed MG does not result in a cell fate shift; SOX2-deficient MG retain their gross morphology, continue to express specific glial markers, and do not reenter the cell cycle. Additionally, this work highlights the essential role that glial scaffolding plays in the neural development and function of the retina. See Figure 9 for a visual representation of these data.

Though *Sox2* is ablated at P5 in MG, a striking disruption of Müller and neuronal processes becomes most evident at P25. Extension of MG processes in the *Sox2*^{CONTROL} retina, and the disruption of those processes observed from P15 to P25 in the *Sox2*^{MUTANT} retina, is likely to directly follow the period of robust synaptogenesis in the retina.^{19,34,43–48} Glial sheaths are known to form around active synapses and, in many regions of the nervous system, glia play an active role in synaptogenesis.^{49–52} Glial sheaths have also been shown in the chick retina to compartmentalize GC processes. Cultures of MG endfeet induced the formation of GC axons, while MG cell bodies promote dendritic growth.⁵³ In the zebrafish retina, photoreceptor circuits are established well before MG lamellar processes reach them.⁵⁴ Interestingly, it has been suggested that the onset of neuronal activity may guide or stimulate the MG outgrowth, possibly through the local influx of K⁺ across MG membranes.^{19,54} These light-evoked K⁺ currents are specifically localized to the synaptic plexiform layers,⁵⁵ where the MG morphology shows the greatest degree of disruption in the *Sox2*^{MUTANT}.

In addition to the observed structural abnormalities, there is a decrease in the b-wave amplitude in the *Sox2*^{MUTANT}, indicating a deficit in retinal function. It is known that the b-wave arises from an ensemble response of retinal cells. ON bipolar cells are a major contributor to the b-wave of the electroretinogram.^{56–58} Studies have also demonstrated that a component of the b-wave is Müller glial in origin.⁵⁹ For example, deletion of the MG-specific water channel, Aquaporin-4, results in a reduction in b-wave amplitude⁶⁰ similar to the phenotype in the *Sox2*^{MUTANT} retinas. Further, adeno-associated virus-mediated, optogenetic ablation of a subset of MG leads to a reduction in b-wave amplitude.⁶¹ However, the global changes in retinal organization observed in both the inner and outer retina in the *Sox2*^{MUTANT} make it challenging to isolate a single factor responsible for this phenotype. Nevertheless, our results further define a critical role for Müller glia in the proper transmission of neuronal signals in the retina.

A New Role for SOX2 in Retinal Maturation

These data describe a new role for SOX2 in postnatal retinal maturation. Our laboratory and others have established that SOX2 is required at all major stages of retinal development for the proper formation of the mammalian eye.^{15,16,27,62} Here, we demonstrate that loss of SOX2 at P5 in a committed glial population results in the abnormal development of processes and adhesion sites throughout the retina. Amacrine cells are the only other population of cells in the retina to constitutively express SOX2. During retinal maturation, it was recently demonstrated that loss of SOX2 in a committed but immature

amacrine cell population also results in aberrant process development.³³ Together, these results suggest that, SOX2 plays an essential role in the positioning of neural and glial cell processes and in the development of dendritic stratification in the postnatal retina. One possible explanation of our results is that ablation of *Sox2* at P5 in Müller glia results in the disruption of the ability of MG to adhere correctly to neural processes in the plexiform layers and to form the zonula adherens junctions between MG and photoreceptor cell bodies, via alteration of expression or localization of these proteins. SOX2 has been linked to N-cadherin expression in the developing lens.⁶³ Both N-cadherin and N-CAM have been shown to be important in MG-neuronal adhesion.^{64,65} Further studies are warranted to explore this possibility.

Together, these data establish a role for SOX2 in the maturation of MG processes and provide new insights into the role of SOX2 in the development of retinal cytoarchitecture. The structural and functional disruption of neuronal and glial architecture at postnatal stages also highlights the extended period of dynamic maturation of the mammalian retina. Understanding the functional and structural plasticity of the postnatal and mature retina is essential for understanding mechanisms of retinal regeneration and considering therapeutic regenerative strategies for the neural retina.

Acknowledgments

The authors thank Eva S. Anton, PhD, Natalia Surzenko, PhD, and Shoji Osawa, PhD, for evaluating the manuscript; Ying Hao and the Duke Eye Center Morphology and Image Processing Module for assistance with electron microscopy; Vladimir Ghukasyan, PhD, and the Neuroscience Center Confocal and Multiphoton Imaging Core; Jeremy Nathans, PhD, for donating the GLASTCreER mice; and Jindong Ding, PhD, and Richard Weinberg, PhD, for insights on the EM data.

The authors dedicate this work to the memory of Larysa H. Pevny (1965–2012). For her wisdom, insight, guidance, and enduring encouragement, we are continually grateful and inspired.

Supported by National Institutes of Health Grants R01EY012224, R01EY022341 (LHP, ERW) and from the Duke Core Grant for Vision Research (P30EY05722). The authors alone are responsible for the content and writing of the paper.

Disclosure: **A.R. Bachleda**, None; **L.H. Pevny**, None; **E.R. Weiss**, None

References

- Turner DL, Cepko CL. A common progenitor for neurons and glia persists in rat retina late in development. *Nature*. 1987; 328:131–136.
- Livesey FJ, Cepko CL. Vertebrate neural cell-fate determination: lessons from the retina. *Nat Rev Neurosci*. 2001;2:2109–118.
- Ohsawa R, Kageyama R. Regulation of retinal cell fate specification by multiple transcription factors. *Brain Res*. 2008;1192:90–98.
- Bringmann A, Pannicke T, Grosche J, et al. Müller cells in the healthy and diseased retina. *Prog Retin Eye Res*. 2006;25:397–424.
- Young RW. Cell differentiation in the retina of the mouse. *Anat Rec*. 1985;212:199–205.
- Zappone MV, Galli R, Catena R, et al. Sox2 regulatory sequences direct expression of a (beta)-Geo transgene to telencephalic neural stem cells and precursors of the mouse embryo, revealing regionalization of gene expression in CNS stem cells. *Development*. 2000;127:2367–2382.
- Bylund M, Andersson E, Novitsch BG, Muhr J. Vertebrate neurogenesis is counteracted by Sox1-3 activity. *Nat Neurosci*. 2003;6:1162–1168.
- D'Amour KA, Gage FH. Genetic and functional differences between multipotent neural and pluripotent embryonic stem cells. *Proc Natl Acad Sci U S A*. 2003;100:11866–11872.
- Graham V, Khudyakov J, Ellis P, Pevny L. SOX2 functions to maintain neural progenitor identity. *Neuron*. 2003;39:749–765.
- Roesch K, Jadhav AP, Trimarchi JM, et al. The transcriptome of retinal Müller glial cells. *J Comp Neurol*. 2008;509:225–238.
- Dyer MA, Cepko CL. Control of Müller glial cell proliferation and activation following retinal injury. *Nat Neurosci*. 2000;3: 873–880.
- Ooto S, Akagi T, Kageyama R, et al. Potential for neural regeneration after neurotoxic injury in the adult mammalian retina. *Proc Natl Acad Sci U S A*. 2004;101:13654–13659.
- Das AV, Mallya KB, Zhao X, et al. Neural stem cell properties of Müller glia in the mammalian retina: regulation by Notch and Wnt signaling. *Dev Biol*. 2006;299:283–302.
- Karl MO, Hayes S, Nelson BR, Tan K, Buckingham B, Reh TA. Stimulation of neural regeneration in the mouse retina. *Proc Natl Acad Sci U S A*. 2008;105:19508–19513.
- Matsushima D, Heavner W, Pevny LH. Combinatorial regulation of optic cup progenitor cell fate by SOX2 and PAX6. *Development*. 2011;138:443–454.
- Surzenko N, Crowl T, Bachleda A, Langer L, Pevny L. SOX2 maintains the quiescent progenitor cell state of postnatal retinal Müller glia. *Development*. 2013;140:1445–1456.
- Reichenbach A, Schneider H, Leibnitz L, Reichelt W, Schaaf P, Schümann R. The structure of rabbit retinal Müller (glial) cells is adapted to the surrounding retinal layers. *Anat Embryol (Berl)*. 1989;180:71–79.
- García M, Vecino E. Role of Müller glia in neuroprotection and regeneration in the retina. *Histol Histopathol*. 2003;18:1205–1218.
- Reichenbach A, Reichelt W. Postnatal development of radial glial (Müller) cells of the rabbit retina. *Neurosci Lett*. 1986;71: 125–130.
- Reichenbach A, Schneider H, Leibnitz L, Reichelt W, Schaaf P, Schümann R. The structure of rabbit retinal Müller (glial) cells is adapted to the surrounding retinal layers. *Anat Embryol (Berl)*. 1989;180:71–79.
- Willbold E, Rothermel A, Tomlinson S, Layer PG. Müller glia cells reorganize reorganizing chicken retinal cells into correctly laminated in vitro retinæ. *Glia*. 2000;29:45–57.
- Poitry-Yamate CL, Poitry S, Tsacopoulos M. Lactate released by Müller glial cells is metabolized by photoreceptors from mammalian retina. *J Neurosci*. 1995;15:5179–5191.
- Newman EA, Zahs KR. Modulation of neuronal activity by glial cells in the retina. *J Neurosci*. 1998;18:4022–4028.
- Reichenbach A, Bringmann A. New functions of Müller cells. *Glia*. 2013;61:651–678.
- Goldman D. Müller glial cell reprogramming and retina regeneration. *Nat Rev Neurosci*. 2014;15:431–442.
- Labin AM, Safuri SK, Ribak EN, Perlman I. Müller cells separate between wavelengths to improve day vision with minimal effect upon night vision. *Nat Commun*. 2014;5:4319.
- Taranova OV, Magness ST, Fagan BM, et al. SOX2 is a dose-dependent regulator of retinal neural progenitor competence. *Genes Dev*. 2006;20:1187–1202.
- Nathans J. Generation of an inducible Slc1a3-cre/ERT transgenic allele. 2010;MGI J:157151. Available at: <http://www.informatics.jax.org/reference/J:157151>.
- de Melo J, Miki K, Rattner A, et al. Injury-independent induction of reactive gliosis in retina by loss of function of

- the LIM homeodomain transcription factor Lhx2. *Proc Natl Acad Sci U S A*. 2012;109:4657-4662.
30. Wang Y, Rattner A, Zhou Y, Williams J, Smallwood PM, Nathans J. *Norrin*/Frizzled4 signaling in retinal vascular development and blood brain barrier plasticity. *Cell*. 2012;151:1332-1344.
 31. Soriano P. Generalized lacZ expression with the ROSA26 Cre reporter strain. *Nat Genet*. 1999;21:70-71.
 32. Das SR, Bhardwaj N, Kjeldbye H, Gouras P. Müller cells of chicken retina synthesize 11-cis-retinol. *Biochem J*. 1992; 285(pt 3):907-913.
 33. Whitney IE, Keeley PW, St John AJ, Kautzman AG, Kay JN, Reese BE. Sox2 regulates cholinergic amacrine cell positioning and dendritic stratification in the retina. *J Neurosci*. 2014;34: 10109-10121.
 34. Fisher LJ. Development of synaptic arrays in the inner plexiform layer of neonatal mouse retina. *J Comp Neurol*. 1979;187:359-372.
 35. Joly S, Pernet V, Samardzija M, Grimm C. Pax6-positive Müller glia cells express cell cycle markers but do not proliferate after photoreceptor injury in the mouse retina. *Glia*. 2011;59: 1033-1046.
 36. Fischer AJ, Zelinka C, Scott MA. Heterogeneity of Glia in the Retina and Optic Nerve of Birds and Mammals. *PLoS One*. 2010;5:e10774.
 37. Kolb H. Glial cells of the retina. *Webvision*. Available at: <http://webvision.med.utah.edu/book/part-ii-anatomy-and-physiology-of-the-retina/glia/glia-cells-of-the-retina/>. Accessed February 5, 2016.
 38. Haverkamp S, Wässle H. Immunocytochemical analysis of the mouse retina. *J Comp Neurol*. 2000;424:1-23.
 39. Ball SL, McEnery MW, Yunker AMR, Shin H-S, Gregg RG. Distribution of voltage gated calcium channel β subunits in the mouse retina. *Brain Res*. 2011;1412:1-8.
 40. Masland RH. The neuronal organization of the retina. *Neuron*. 2012;76:266-280.
 41. Lewis GP, Linberg KA, Fisher SK. Neurite outgrowth from bipolar and horizontal cells after experimental retinal detachment. *Invest Ophthalmol Vis Sci*. 1998;39:424-434.
 42. Strettoi E, Porciatti V, Falsini B, Pignatelli V, Rossi C. Morphological and functional abnormalities in the inner retina of the rd/rd mouse. *J Neurosci*. 2002;22:5492-5504.
 43. Olney JW. An electron microscopic study of synapse formation, receptor outer segment development, and other aspects of developing mouse retina. *Invest Ophthalmol Vis Sci*. 1968;7:250-268.
 44. Blanks JC, Adinolfi AM, Lolley RN. Synaptogenesis in the photoreceptor terminal of the mouse retina. *J Comp Neurol*. 1974;156:81-93.
 45. Sherry DM, Wang MM, Bates J, Frishman IJ. Expression of vesicular glutamate transporter 1 in the mouse retina reveals temporal ordering in development of rod vs. cone and ON vs. OFF circuits. *J Comp Neurol*. 2003;465:480-498.
 46. Meister M, Wong RO, Baylor DA, Shatz CJ. Synchronous bursts of action potentials in ganglion cells of the developing mammalian retina. *Science*. 1991;252:939-943.
 47. Penn AA, Wong RO, Shatz CJ. Neuronal coupling in the developing mammalian retina. *J Neurosci*. 1994;14:3805-3815.
 48. Wong ROL. Retinal waves and visual system development. *Annu Rev Neurosci*. 1999;22:29-47.
 49. Ullian EM, Sapperstein SK, Christopherson KS, Barres BA. Control of synapse number by glia. *Science*. 2001;291:657-661.
 50. Christopherson KS, Ullian EM, Stokes CCA, et al. Thrombospondins are astrocyte-secreted proteins that promote CNS synaptogenesis. *Cell*. 2005;120:421-433.
 51. Allen NJ, Bennett ML, Foo LC, et al. Astrocyte glypicans 4 and 6 promote formation of excitatory synapses via GluA1 AMPA receptors. *Nature*. 2012;486:410-414.
 52. Corty MM, Freeman MR. Architects in neural circuit design: Glia control neuron numbers and connectivity. *J Cell Biol*. 2013;203:395-405.
 53. Bauch H, Stier H, Schlosshauer B. Axonal versus dendritic outgrowth is differentially affected by radial glia in discrete layers of the retina. *J Neurosci*. 1998;18:1774-1785.
 54. Williams PR, Suzuki SC, Yoshimatsu T, et al. In vivo development of outer retinal synapses in the absence of glial contact. *J Neurosci*. 2010;30:11951-11961.
 55. Karwoski CJ, Newman EA, Shimazaki H, Proenza LM. Light-evoked increases in extracellular K⁺ in the plexiform layers of amphibian retinas. *J Gen Physiol*. 1985;86:189-213.
 56. Gurevich L, Slaughter MM. Comparison of the waveforms of the ON bipolar neuron and the b-wave of the electroretinogram. *Vision Res*. 1993;33:2431-2435.
 57. Masu M, Iwakabe H, Tagawa Y, et al. Specific deficit of the ON response in visual transmission by targeted disruption of the mGluR6 gene. *Cell*. 1995;80:757-765.
 58. Tian N, Slaughter MM. Correlation of dynamic responses in the ON bipolar neuron and the b-wave of the electroretinogram. *Vision Res*. 1995;35:1359-1364.
 59. Frishman IJ. Chapter 7 - electrogenesis of the electroretinogram. In: Ryan SJ, ed. *Retina*. 5th ed. London: W.B. Saunders; 2013:177-201. Available at: <http://www.sciencedirect.com/science/article/pii/B9781455707379000072>. Accessed August 17, 2015.
 60. Li J, Patil RV, Verkman AS. Mildly abnormal retinal function in transgenic mice without Müller cell aquaporin-4 water channels. *Invest Ophthalmol Vis Sci*. 2002;43:573-579.
 61. Byrne LC, Khalid F, Lee T, et al. AAV-mediated, optogenetic ablation of Müller glia leads to structural and functional changes in the mouse retina. *PLoS One*. 2013;8:e76075.
 62. Langer L, Taranova O, Sulik K, Pevny L. SOX2 hypomorphism disrupts development of the prechordal floor and optic cup. *Mech Dev*. 2012;129:1-12.
 63. Kamachi Y, Uchikawa M, Tanouchi A, Sekido R, Kondoh H. Pax6 and SOX2 form a co-DNA-binding partner complex that regulates initiation of lens development. *Genes Dev*. 2001;15: 1272-1286.
 64. Drazba J, Lemmon V. The role of cell adhesion molecules in neurite outgrowth on Müller cells. *Dev Biol*. 1990;138:82-93.
 65. Tepass U, Truong K, Godt D, Ikura M, Peifer M. Cadherins in embryonic and neural morphogenesis. *Nat Rev Mol Cell Biol*. 2000;1:91-100.